EXPERIMENTS OF CRYSTAL BALL COLLABORATION AT BNL

PNPI participants of the Crystal Ball Collaboration:
V.V. Abaev, V.S. Bekrenev, N.G. Kozlenko, S.P. Kruglov, A.A. Kulbardis, I.V. Lopatin, A.B. Starostin

1. Introduction

The experimental program "Baryon spectroscopy with the Crystal Ball" was under way in 1998–2002 at the Alternating Gradient Synchrotron AGS of Brookhaven National Laboratory, USA. The main goal of this program was to map up the existence of all baryon resonances and to study their characteristics with a high precision. The program has been carried out with the team, the Crystal Ball Collaboration, including 14 institutions from 5 countries. Physicists of PNPI participated in this collaboration playing an essential role.

Almost all our information on the N and Δ resonances comes from πN data, mainly from elastic scattering, in the form of cross section and polarization measurements. The data are synthesized by a partial-wave analysis. The end products are the various partial waves; the Argand diagram and speed plot of each wave are used to identify the resonances. Till starting the experiments at BNL, the πN data sets in certain energy regions were incomplete and it was easy for a resonance with a small elasticity to be missed. One of the most evident shortcomings of the existed data-base was a lack of precise and systematic data on $\pi^- p$ reaction with neutral particles in the final state: $\pi^- p \to \gamma n$, $\pi^- p \to \pi^0 n$, $\pi^- p \to \pi^0 \pi^0 n$, $\pi^- p \to \eta n$.

The experiment E913 at the AGS was concerned with the systematic measurement of neutral final states in $\pi^- p$ interactions in the region of low-lying πN resonances; the experiment covered the N and Δ resonances using π^--beams.

The multi-photon Crystal Ball detector was used for registering photons and neutral mesons in this experiment. This detector has a good energy and angular resolution. The Crystal Ball made it possible to study neutral baryon spectroscopy on a scale not seen before.

2. The Crystal Ball detector

The Crystal Ball is a highly segmented, total absorption electromagnetic calorimeter and spectrometer, covering over 94% of 4π steradian. The Crystal Ball detector was installed at the C6 beam line of the AGS at Brookhaven National Laboratory. The ball proper is a sphere with an entrance and exit opening for the beam and an inside cavity for the target. The ball (see Fig. 1) is constructed of 672 optically isolated NaI(Tl) crystals, 15.7 radiation length thick. Each crystal is viewed by its own photomultiplier tube.

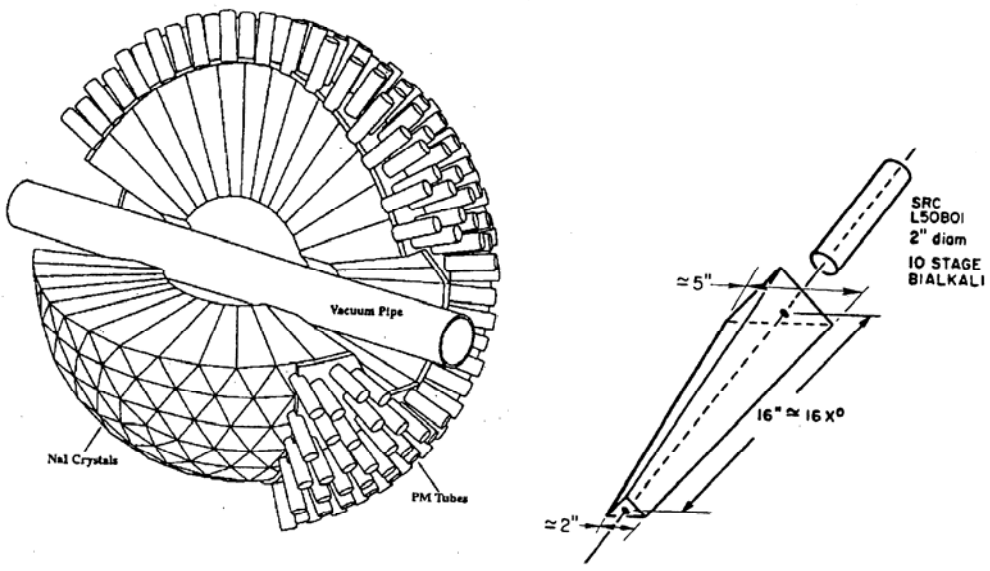

Fig. 1. Left: the Crystal Ball detector. Right: the typical Crystal Ball crystal

The counters are arranged in a spherical shell with an inner radius of 25.3 cm and an outer radius of 66 cm. The sphere is approximated by an icosahedron, a figure consisting of 20 equivalent equilateral triangles called as "major" triangles. Each major triangle is divided into 4 "minor" triangles and each minor triangle consists of 9 crystals. While majors are similar, there are 2 types of minors – the central minor is slightly different from the corners. The Crystal Ball consists of 11 types of slightly different shaped crystals. The crystals are about 41 cm long truncated triangular pyramids about 14 cm across at the outer and about 5 cm at the inner radius.

An electromagnetic shower from a single photon deposits energy in several crystals, called a cluster. The present cluster algorithm sums the energy from the crystal with the highest energy with that from the twelve nearest neighbors. Shower directions are measured with the resolution in polar angle $\sigma_\theta = 2^\circ$–3° for energies in the range 50–500 MeV; the resolution in azimuthal angle is $\sigma_\varphi = 2^\circ/\sin\theta$. The energy resolution was $\sigma_E/E = 2.0\%/E^{0.36}$ with E given in GeV. The Crystal Ball is also ia useful detector of neutrons. Neutrons with a kinetic energy of 10–250 MeV are detected with an efficiency of 20–40%.

A liquid hydrogen target LH_2 (a 10 cm diameter horizontal cylinder with spherical endcaps and total thickness along the beam axis being equal to 10.56 cm) was installed inside a vacuum pipe. A veto barrel consisting of four 120 cm long plastic scintillation counters surrounding the vacuum pipe was used to identify neutral (no signal in the veto barrel) and charged (at least one veto barrel signal) triggers.

In an experiment, the coordinates and momenta of beam particles were determined using a set of seven drift chambers. Three drift chambers were used to measure the horizontal coordinates, three chambers were used to measure the vertical coordinates and one chamber situated upstream of the beam bending magnet aimed to determine the beam particle's momentum. An eight element horizontal hodoscope was mounted immediately upstream of the first drift chamber at the point of maximum horizontal momentum dispersion of the beam.

3. Study of $\pi^- p$ charge exchange scattering $\pi^- p \to \pi^0 n$

In experiments with the liquid hydrogen target over 42×10^6 triggers for $\pi^- p \to$ *neutrals* were collected at 22 beam momenta over a range of 150–760 MeV/c; additional runs with an empty target were taken at each momentum. This momentum range includes four low-lying resonances: $P_{33}(1232)$, $P_{11}(1440)$, $D_{13}(1520)$ and $S_{11}(1535)$.

When studying the $\pi^- p$ charge exchange (CEX) reaction, two- and three-cluster events were used to select this reaction and to calculate differential cross sections. The π^0 meson from the CEX reaction decays into two photons immediately, and the showers from these two photons give clusters in the Crystal Ball NaI(Tl) crystals. The cluster finding program finds the crystal with maximum deposited energy, adds the energies from adjoining crystals and then zeroes the energies in those crystals. After that the program finds the next crystal with the maximum energy to form the next cluster and so on until all the clusters are found. Events containing clusters with the maximum energy in a crystal at the beam entrance or exit holes were rejected. For two-cluster events the invariant mass was calculated in assumption that both clusters are from photons. If the invariant mass coincides with the mass of π^0 meson and the kinematics of the CEX reaction is fulfilled, then the event was accepted. For three-cluster events the analysis is more complicated – it is not known which cluster is produced by the neutron, so all possible combinations must be examined.

The Crystal Ball acceptance was determined on the base of the Monte Carlo simulation of the experiment. The acceptance value rapidly decreased when $\cos\theta_{cm} > 0.5$ because of the beam-exit tunnel.

At the first stage of data processing, results for the CEX reaction $\pi^- p \to \pi^0 n$ are obtained for eight momenta in the range from 147 to 322 MeV/c [1, 2]; the momentum spread (σ) varied from 1.5% to 1.0%, respectively. When carrying out the experiment, the beam contamination was determined using the time-of-flight (TOF) technique on the base of about 9 meters. As an example, the μ/π fraction was evaluated to be 3.5% and e/π was 5.9% at 300 MeV/c using this technique.

As a result of data processing, the center-of-mass scattering angle θ_{cm} was calculated for each CEX event and the data were histogrammed into 20 bins $\Delta\cos\theta_{cm} = 0.1$. Yields taken with the empty target were

subtracted then from the data taken with the full target, and the differential cross sections were calculated at each angular bin. In total, 160 new experimental points were obtained. The statistical errors are typically 2–6% except forward-angle points at three lowest momenta where the cross sections decrease to a few tenths of millibarn. Systematic uncertainties increase from 3% to 6.5% as the beam momentum decreases.

The differential cross sections were integrated to obtain the total charge-exchange cross sections at eight momenta. In Fig. 2 the results are presented in comparison with the predictions of the FA02 partial-wave analysis (PWA) and with previous data. As with the differential cross sections, the total cross sections are in a good agreement with the FA02 PWA.

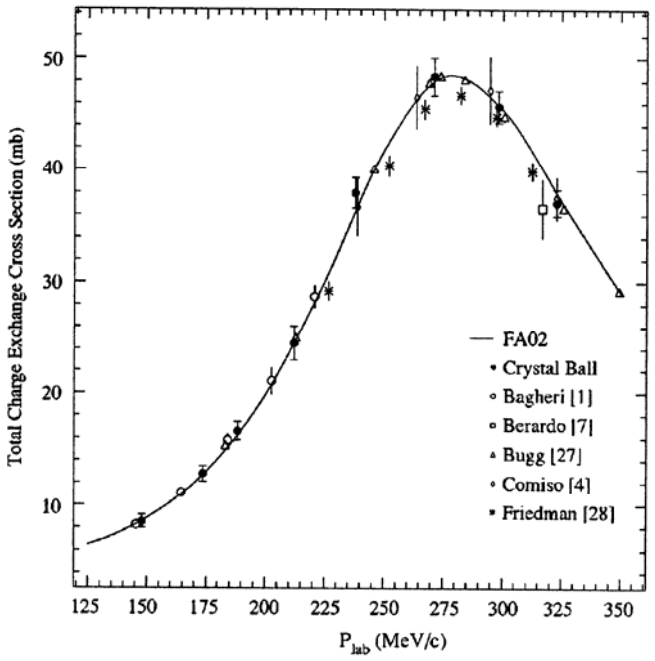

Fig. 2. The total cross sections obtained from integrating the differential cross sections. The results are compared to the FA02 PWA and to previous data

At the next stage of data processing, the differential cross sections of the CEX reaction were obtained [3] for momenta in the vicinity of the η-production threshold – from p_π = 649 MeV/c to 752 MeV/c. Since the TOF-technique is not appropriate to determine lepton contamination in the beam in such high momenta, a cylindrical gas Cherenkov counter was used to measure the electron contamination. This experiment used a pion beam with a momentum spread of $\sigma \approx 1\%$. The momentum dispersion of the beam on the hodoscope plane was used to split the beam distribution into narrower momentum intervals, which have a typical resolution of $\sigma \approx 5$ MeV. Each fraction of the beam passing through one of the hodoscope counters was analyzed independently. The mean value of the beam momentum for each individual hodoscope counter was obtained from the momentum spectrometer. As a result, the differential cross sections of the CEX reaction were calculated in 27 momentum bins. The full covered angular range (from –1 to +1 in $\cos\theta_{cm}$) was divided into 24 angular bins. In total, 648 new experimental points were obtained in this experiment. A value of the statistical error varies from 5% to 15% – depending on the momentum and angle. The overall systematic uncertainty that affects the normalization of the differential cross sections is estimated to be 4% for the momenta below 689 MeV/c and 6% for the momenta above.

Shown in Fig. 3 are three examples of the CEX differential cross sections. A comparison is made with the predictions of the FA02 PWA. There is good agreement between the PWA results and experimental data at p_π = 661 MeV/c and p_π = 705 MeV/c. The PWA results agree with our data at these momenta in both the absolute magnitude and the shape of the distribution over the full angular range. At p_π = 742 MeV/c, the PWA results deviate from our data by 10–15% at backward angles.

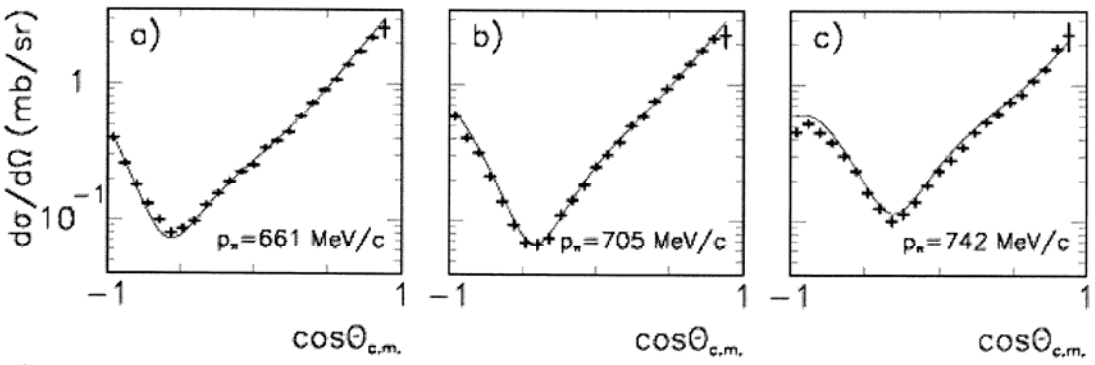

Fig. 3. The differential cross sections of the CEX reaction at selected momenta compared to the FA02 PWA (solid line). The ordinates of the histograms are logarithmic

In 2002, a separate experiment was carried out in which the liquid hydrogen target was replaced with a thin polyethylene (CH_2) target, 10 cm in diameter; the monitor counter was placed immediately in front of this target. Several data sets were obtained with both CH_2 and carbon (C) targets at nine incident beam momenta between 547 and 750 MeV/c. When carrying out this experiment, a lead plate of 3-mm thickness was inserted upstream of the second dipole magnet to eliminate most of electron component by radiation losses, so the electron contamination for the CH_2 – C data (measured using the gas Cherenkov counter) was about 6%.

The differential cross sections for CH_2 – C were calculated after subtracting the normalized carbon data from the CH_2 data. The typical carbon contribution was 30%. For calculating the differential cross sections the full angular range (from –1 to +1 in $\cos\theta_{cm}$) was divided into 24 angular bins. In total, about 200 new experimental points were obtained [4]. The statistical errors are at a level of 5–15%, the systematic uncertainties are estimated to be equal to 6%. A comparison of obtained differential cross sections with the predictions of the FA02 PWA shows their general agreement within 5%, although remarkable deviations are observed at momenta higher than 675 MeV/c and at angles $\cos\theta_{cm} < -0.45$ – see Fig. 4.

At the beam momentum of 720 MeV/c the differential cross sections were obtained in measurements with both the liquid hydrogen and polyethylene targets – the electron contamination in the beam was 6% in both cases. A comparison shows that the results agree within 3%.

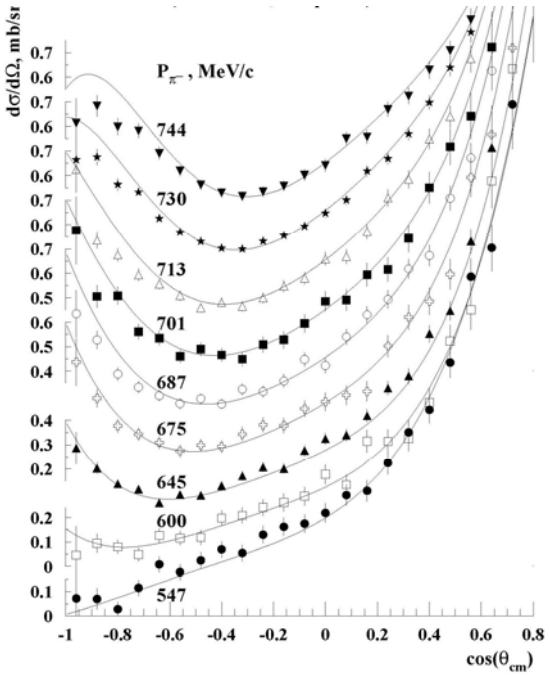

Fig. 4. The differential cross sections of the CEX reaction measured using the CH_2 target. Shown by curves are the predictions of the FA02 PWA

4. Study of the η-production process $\pi^- p \to \eta n$

At the incident pions momenta higher than the η-production threshold accumulated data were used to obtain cross sections of the reaction $\pi^- p \to \eta n$. Until now existing experimental information on the cross sections of this reaction has been very scarce and contradictory, especially near the threshold. At the same time, obtaining accurate experimental data in the near-threshold region is very important for verifying theoretical models of η-production. Such data will also be useful for extracting the ηN scattering length and understanding properties of the $S_{11}(1535)$ resonance.

Cross sections of the reaction $\pi^- p \to \eta n$ were determined in the momentum range from the threshold (685 MeV/c) up to 750 MeV/c. The η meson produced in this reaction has – as distinct from the $\pi^- p$ charge exchange scattering – two decay modes with approximately equal branching ratios: $\eta \to \gamma\gamma$ and $\eta \to 3\pi^0$. Evidently, in this case the candidates for the $\pi^- p \to \eta n \to 2\gamma n$ and $\pi^- p \to \eta n \to 3\pi^0 n \to 6\gamma n$ channels are the neutral two-cluster and six-cluster events, respectively, assuming that each cluster is because of a photon shower in the Crystal Ball. The neutron is assumed to be the missing particle. Because the $\pi^- p \to \eta n$ reaction is studied near the production threshold, only a few percent of all events have the final-state neutron entering the crystals of the Crystal Ball, *i.e.* almost all events have the neutrons escaping through the downstream tunnel. So events in which there was an extra cluster from a neutron were not taken into account.

At the first stage of data processing, only events caused by the $\eta \to \gamma\gamma$ decay were considered – see Refs. [5, 6]. Both the differential and total cross sections were obtained as a result of this work. The differential cross sections were fitted with Legendre polynomials: $d\sigma/d\Omega = a_0 + a_1 P_1(\cos\theta_{cm}) + a_2 P_2(\cos\theta_{cm})$. It appeared that at momenta up to 705 MeV/c the *S*-wave amplitude gives the main contribution to the cross sections, while for momenta from 705 to 750 MeV/c the contribution of higher waves becomes essential. The total cross sections obtained by integrating $d\sigma/d\Omega$ are in a general agreement with results of previous experiments but exceed them in statistical accuracy.

More detailed data analysis was performed some later [7]. The two sets of results for the differential cross sections for the reaction $\pi^- p \to \eta n$ using $\eta \to \gamma\gamma$ and $\eta \to 3\pi^0$ decays are shown in Fig. 5.

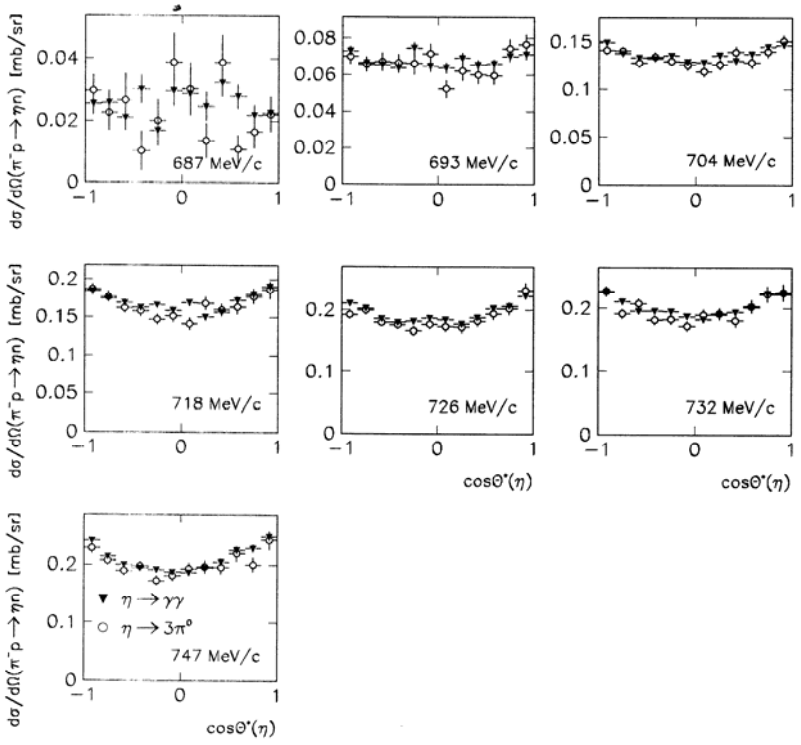

Fig. 5. Differential cross sections for $\eta \to \gamma\gamma$ (filled triangles) and $\eta \to 3\pi^0$ (open circles) decays

Inspection of this figure reveals that results obtained using $\eta \to \gamma\gamma$ decay is smoother than ones obtained using $\eta \to 3\pi^0$. This can be explained by the fact that the number of $\eta \to \gamma\gamma$ decays detected in the Crystal Ball is 3.5 times the number of $\eta \to 3\pi^0$ ones.

The systematic uncertainty in $d\sigma/d\Omega$ is dominated by two sources: the uncertainty in the η decay branching ratio and the uncertainty in the determination of the lepton contamination of the incident π^- beam. The absolute uncertainty in the value of $BR(\eta \to \gamma\gamma)$, which has been determined directly, is only 0.9%. In contrast, $BR(\eta \to 3\pi^0)$ has been determined only relatively. For this reason, authors of Ref. [7] preferred to use the $d\sigma/d\Omega$ data set obtained using $\eta \to \gamma\gamma$ rather than taking the weighted average of the two sets. As to the systematic uncertainty in the determination of the lepton contamination in the beam, it was taken to be 6% – in accordance with the procedure described in Ref. [3].

The $d\sigma/d\Omega$ angular distribution for two lowest momenta looks isotropic confirming that near the threshold the η-production process goes through formation of the $S_{11}(1535)$ resonance. For $p_\pi \geq 704$ MeV/c these angular distributions are bowl shaped. This is consistent with no *P*-wave and a modest *D*-wave production of order 5–10% and *S*-*D* interference. This conclusion coincides with that made in Refs. [5, 6].

The total cross section increases immediately and rapidly from the η-production threshold at 685 MeV/c, reaching 2.6 mb at $p_\pi = 750$ MeV/c.

3. Study of forbidden and rare decays of η meson

The Crystal Ball collected approximately 30×10^6 η mesons from the reaction $\pi^- p \to \eta n$ using a liquid hydrogen target at a beam momentum of 720 MeV/c.

An important goal of this experiment was to improve the present values of branching ratios for rare and forbidden decays of the η meson. Besides the most intense neutral decays $\eta \to 2\gamma$ and $\eta \to 3\pi^0$ having branching ratios of 39.4% and 32.5%, accordingly, the following neutral decay modes forbidden for different reasons were investigated using the Crystal Ball: $\eta \to 3\gamma$, $\eta \to \pi^0\gamma$, $\eta \to 2\pi^0\gamma$, $\eta \to 3\pi^0\gamma$, $\eta \to 4\pi^0$.

The decay $\eta \to 3\gamma$ is forbidden by *C* invariance. Besides, there exist several additional factors which suppress this decay. The decay to three photons is an electromagnetic interaction of the 3rd order proportional to $\alpha^3 \approx 4 \times 10^{-7}$. The decay is suppressed even more by the limitations of the phase space and by the centrifugal barrier. The upper limit for this decay measured in this experiment for the first time is $BR(\eta \to 3\gamma) < 4 \times 10^{-5}$ at the 90% CL [8]. Candidates for the $\pi^- p \to \eta n \to 3\gamma n$ process were searched for in the three-cluster data set, which comprised 18.4×10^6 events. The mostly significant experimental background is due to the decay $\eta \to 3\pi^0 \to 6\gamma$, when photon showers overlap in the detector.

A spin-zero to spin-zero transition by the emission of a real photon is forbidden by conservation of angular momentum. Thus, the decay mode $\eta \to \pi^0\gamma$ should be absolutely forbidden. Furthermore, this decay is not allowed by gauge invariance and by *C* invariance. Possible candidates for the $\pi^- p \to \eta n \to \pi^0\gamma n \to 3\gamma n$ process were searched for in the same three-cluster data set that was used for the determination of the upper limit in $BR(\eta \to 3\gamma)$. This process has the same background sources as the $\pi^- p \to \eta n \to 3\gamma n$ process. The number of effective constraints that apply to the $\pi^- p \to \pi^0\gamma n \to 3\gamma n$ hypothesis is one more than for $\pi^- p \to 3\gamma n$, namely the mass of the π^0 meson. The obtained upper limit $BR(\eta \to \pi^0\gamma) < 9 \times 10^{-5}$ at the 90% CL [8] is about two times larger than the one for $BR(\eta \to 3\gamma)$.

The decay modes $\eta \to 2\pi^0\gamma$ and $\eta \to 3\pi^0\gamma$ are strictly forbidden both by charge conjugation invariance. The five-cluster data set of 5.2×10^6 events was used to search for $\pi^- p \to \eta n \to 2\pi^0\gamma n \to 5\gamma n$ candidates. The background for this decay is determined mainly by evens from the decay $\eta \to 3\pi^0$ in cases when two single-photon showers overlap or one photon is not detected in the Crystal Ball. Another source of background is the reaction $\pi^- p \to 2\pi^0 n$ when either a single-photon splits off or the neutron is detected in the Crystal Ball. The obtained upper limit is $BR(\eta \to 2\pi^0\gamma) < 5 \times 10^{-4}$ at the 90% CL [9]. Using the value $\Gamma(\eta \to all) = 1.29 \pm 0.07$ keV, the *BR* was converted to the decay-width upper limit: $\Gamma(\eta \to 2\pi^0\gamma) < 0.64$ eV. No searches for this decay mode have been reported earlier. To search for the reaction $\pi^- p \to \eta n \to 3\pi^0\gamma n \to 7\gamma n$ the sample of seven-cluster events was used, which has 0.168×10^6 entries. The main source of background here is $\eta \to 3\pi^0 \to 6\gamma$ events with seventh cluster produced by a one-photon shower split-off or an occasional

cluster from a pile-up event. To suppress this background, the several selection cuts were applied. The obtained upper limits are $BR(\eta \to 3\pi^0\gamma) < 6 \times 10^{-5}$ at the 90% CL and $\Gamma(\eta \to 3\pi^0\gamma) < 0.077$ eV [10].

The decay $\eta \to 4\pi^0$ is forbidden by *CP* conservation, so it provided a test for strong *CP*-violating amplitudes down to a level of about 10^{-7} where weak interactions come into play. This decay mode requires 8 neutral clusters in the Crystal Ball which must be reconstructed to four π^0 mesons which together have the invariant mass of the η meson. This enables also to eliminate the expected background from the $\eta \to 3\pi^0$ decay in which there are two extra clusters from photon showers which breakup into separate clusters. The main limitation of the $4\pi^0$ decay mode is its small phase space, the maximum π^0 momentum in $\eta \to 4\pi^0$ is only 39 MeV/c, as compared to the π^0 momentum in $\eta \to 2\pi^0$ of 238 MeV/c. The eight-cluster data set contained 14804 experimental events. These events were subjected to a constrained least square fit satisfying the $\pi^- p \to \eta n \to 4\pi^0 n \to 8\gamma n$ reaction hypothesis with a confidence level > 2% With no 8-cluster event from $\eta \to 4\pi^0$ found, the upper limits become $BR(\eta \to 4\pi^0) < 6.9 \times 10^{-7}$ at the 90% CL and $\Gamma(\eta \to 4\pi^0) < 8.3 \times 10^{-4}$ eV [10].

All above considered decays of the η meson are forbidden – in the framework of the Standard Model – by the fundamental conservation laws, and a stimulus for the investigation of branching ratios of such decays is the search for such decay mechanisms which were outside the Standard Model. However, there is another category of decays (so called rare decays) values of branching ratios for which are predicted by existing theoretical models, and experiments on measuring these branching ratios are important for testing these models. The η-meson decays $\eta \to \pi^0\gamma\gamma$, $\eta \to \pi^0\pi^0\gamma\gamma$ belong just to this category. For example, measurement of the decay rate for $\eta \to \pi^0\gamma\gamma$ is a direct test of the correctness of calculations of the third order χPTh, the first order being zero and the second order being very small. The experimental determination of the $BR(\eta \to \pi^0\gamma\gamma)$ is a rather complicated task, mainly because of the contribution of background from the decay $\eta \to 3\pi^0 \to 6\gamma$ and the reaction $\pi^- p \to 2\pi^0 n \to 4\gamma n$. As a result of multi-step procedure of processing four-cluster data set about 1600 events attributed to the decay $\eta \to \pi^0\gamma\gamma$ were obtained. This gives $BR(\eta \to \pi^0\gamma\gamma) = (3.5 \pm 0.7_{stat} \pm 0.6_{syst}) \times 10^{-4}$ and $\Gamma(\eta \to \pi^0\gamma\gamma) = 0.45 \pm 0.09_{stat} \pm 0.08_{syst}$ eV [11]. This result agrees well with the theoretically calculated value $\Gamma(\eta \to \pi^0\gamma\gamma) = 0.47 \pm 0.10$ eV but lower by a factor of 2 in comparison with the experimental value obtained in 1982 at the setup GAMS.

There are χPTh theoretical predictions for the probability of the decay $\eta \to \pi^0\pi^0\gamma\gamma$, but estimations of the *BR* values given by theoreticians are too low (at a level of 10^{-6}–10^{-7}) to be confirmed or rejected on the base of existing experimental data. For the time present, an analysis of data obtained using the Crystal Ball has given only the upper limit for the *BR* of this decay: $BR(\eta \to \pi^0\pi^0\gamma\gamma) < 1.2 \times 10^{-3}$ [8].

References

1. A.A. Kulbardis for the Crystal Ball Collaboration, in *Proceedings of the 9th International Conference on Hadron Spectroscopy* (Protvino, Russia, 26 August – 1 September 2001), AIP Conference Proceedings, **619**, 701 (2002).
2. M.E. Sadler, A.A. Kulbardis *et al.*, Phys. Rev. C **69**, 055206 (2004).
3. A. Strarostin *et al.*, Phys. Rev. C **72**, 015205 (2005).
4. N.G. Kozlenko *et al.*, Preprint PNPI-2684, Gatchina, 2006. 56 p.
5. N.G. Kozlenko *et al.*, Phys. Atom. Nucl. **66**, 110 (2003).
6. N.G. Kozlenko for the Crystal Ball Collaboration, in *Proceedings of the 9th International Conference on Hadron Spectroscopy* (Protvino, Russia, 26 August – 1 September 2001), AIP Conference Proceedings, **619**, 697 (2002).
7. S. Prakhov *et al.*, Phys. Rev. C **72**, 015203 (2005).
8. B.M.K. Nefkens *et al.*, Phys. Rev. C **72**, 035212 (2005).
9. B.M.K. Nefkens *et al.*, Phys. Rev. Lett. **94**, 041601 (2005).
10. S. Prakhov *et al.*, Phys. Rev. Lett. **87**, 192001 (2000).
11. S. Prakhov *et al.*, Phys. Rev. C **72**, 025201 (2005).